INTERNATIONAL JOURNAL FOR NUMERICAL METHODS IN FLUIDS
Int. J. Numer. Meth. Fluids 2004; **44**:777–788 (DOI: 10.1002/fld.679)

Reference values for drag and lift of a two-dimensional time-dependent flow around a cylinder

Volker John*,†

Otto-von-Guericke-Universität Magdeburg, Institut für Analysis und Numerik, Postfach 4120, 39016 Magdeburg, Germany

SUMMARY

This paper presents a numerical study of a two-dimensional time-dependent flow around a cylinder. Its main objective is to provide accurate reference values for the maximal drag and lift coefficient at the cylinder and for the pressure difference between the front and the back of the cylinder at the final time. In addition, the accuracy of these values obtained with different time stepping schemes and different finite element methods is studied. Copyright © 2004 John Wiley & Sons, Ltd.

KEY WORDS: time-dependent incompressible Navier–Stokes equations; drag coefficient; lift coefficient

1. INTRODUCTION

The Navier–Stokes equations are the fundamental equations of fluid dynamics. Many schemes for their numerical solution have been developed and probably will be developed. These schemes have to be tested at appropriate examples. A common way consists in choosing a velocity–pressure pair $(\mathbf{u}, p)$ and setting the right-hand side and the boundary conditions such that $(\mathbf{u}, p)$ fulfils the Navier–Stokes equations. But a solution $(\mathbf{u}, p)$ chosen in this way has in general no physical meaning. In addition, the typical quantities which are investigated, like errors in norms of Lebesgue or Sobolev spaces, are often not of interest in applications.

It is unlikely to find an analytical description of solutions of real flow problems. Even for academic test examples which try to mimic at least some features of real flows, like the test problem chosen in this paper, analytical solutions are not known generally. There are two ways to provide reference data for such problems. The first one consists in the measurement of quantities of interest in experiments. The second way is to perform careful numerical studies with highly accurate discretizations. The development of high-performance computers in the recent decades made this way feasible. An advantage of this approach is that in the reference data no measurement errors are present. Thus, the use of advanced numerical techniques can

*Correspondence to: V. John, Institut für Analysis und Numerik, Otto-von-Guericke-Universität Magdeburg, Postfach 4120, 39016 Magdeburg, Germany.
†E-mail: john@mathematik.uni-magdeburg.de, url: http://www-ian.math.uni-magdeburg.de/home/john/

Received 9 November 2002
Revised 13 June 2003

provide highly accurate reference data which can be used, e.g. for the validation of codes or for convergence studies of discretizations. Examples of this approach can be found in the literature, e.g. for the stationary Navier–Stokes equations. In Reference [1], reference data for the vortices in a two-dimensional driven cavity problem are obtained in this way. The reattachment point of vortices in a two-dimensional backward facing step problem are computed in Reference [2]. Drag and lift coefficients of a two-dimensional flow around a cylinder are computed very accurately in References [3, 4]. Even for a three-dimensional flow around a cylinder such data are available in Reference [5].

This paper presents a numerical study of a time-dependent two-dimensional flow through a channel around a cylinder. The definition of this test problem is simple such that it can be implemented easily in each code. The flow described by the test problem possesses features which often occur in real flow problems and whose accurate simulation is important in applications, like the formation and separation of eddies.

This test problem has been defined within the DFG high priority program *flow simulation with high-performance computers* in Reference [6]. The goal in Reference [6] was the definition of reference values for the maximum of the drag and lift coefficient at the cylinder and for the difference of the pressure between the front and the back of the cylinder at the final time. The computational results of nine different groups which worked with different codes can be found in Reference [6]. There were codes which used implicit temporal discretizations as well as codes based upon explicit ones. As spatial discretizations finite difference schemes, finite volume schemes or finite element methods were applied. Based on the available numerical results from these groups, the authors of Reference [6] could not define reference values for the above-mentioned parameters but they defined reference intervals, see also Section 4.

In the numerical studies presented in this paper, the underlying Navier–Stokes equations are discretized by an implicit second-order time stepping scheme (fractional-step θ-scheme or Crank–Nicolson scheme) and by an isoparametric second-order finite element discretization (Q_2/P_1^{disc} or P_2/P_1). The computations on the finest grids (6400 time steps, around half a million degrees of freedom in space) allow the definition of reference values for the above-mentioned parameters. This means that the accuracy of the reference data is improved considerably in comparison to Reference [6]. The availability of reference values (instead of reference intervals) simplifies also the assessment of numerical results obtained at the given test problem.

In addition to the definition of the reference values, the accuracy of the results obtained with the different discretizations with various lengths of the time step and on different refinement levels in space is studied.

2. THE TEST PROBLEM

We consider the time-dependent incompressible Navier–Stokes equations

$$\mathbf{u}_t - \nu\Delta\mathbf{u} + (\mathbf{u}\cdot\nabla)\mathbf{u} + \nabla p = \mathbf{f} \quad \text{in } (0,T]\times\Omega$$

$$\nabla\cdot\mathbf{u} = 0 \quad \text{in } [0,T]\times\Omega$$

$$\mathbf{u}(0;x,y) = \mathbf{0} \quad \text{in } \Omega$$

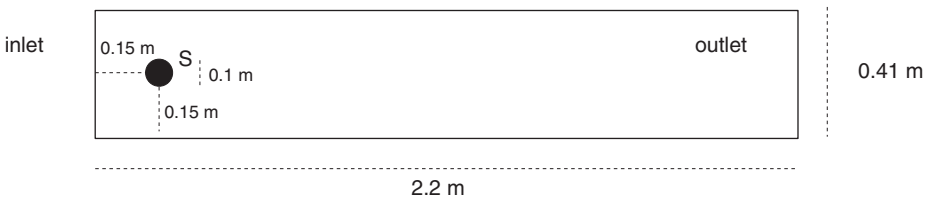

Figure 1. Domain Ω of the test problem.

$$\mathbf{u} = \mathbf{g} \quad \text{in } [0,T] \times \partial\Omega$$

$$\int_\Omega p \, \mathrm{d}x \, \mathrm{d}y = 0 \quad \text{in } (0,T] \tag{1}$$

where Ω is the channel with the cylinder presented in Figure 1, $\nu = 10^{-3}\ \mathrm{m^2\ s^{-1}}$, $\mathbf{f} = \mathbf{0}$ and $T = 8$ s. The time-dependent inflow and outflow profile

$$\mathbf{u}(t;0,y) = \mathbf{u}(t;2.2,y) = 0.41^{-2} \sin(\pi t/8)(6y(0.41 - y), 0)\ \mathrm{m\ s^{-1}}, \quad 0 \leqslant y \leqslant 0.41$$

is prescribed. No-slip conditions are given at the other boundaries. The mean inflow velocity is $U(t) = \sin(\pi t/8)\ \mathrm{m\ s^{-1}}$ such that $U_{\max} = 1\ \mathrm{m\ s^{-1}}$. Based on $U(t)$ and the diameter of the cylinder $L = 0.1$ m, the Reynolds number of the flow is $0 \leqslant Re(t) \leqslant 100$. The density of the fluid is given by $\rho = 1\ \mathrm{kg\ m^{-3}}$. Since the considered problem is two-dimensional, it is well known that a weak solution $(\mathbf{u}, p)$ exists and this solution is unique, e.g. see References [7, 8] for a precise definition of a weak solution and proofs.

The development of the flow is depicted in Figure 2.‡ With increasing inflow, two vortices start to develop behind the cylinder, see $t = 2$ and 4 s. Between $t = 4$ and 5 s, the vortices separate from the cylinder and a vortex street develops. The vortices are still visible at the final time $T = 8$ s.

The parameters of interest are the drag coefficient $c_{\mathrm{d}}(t)$ at the cylinder, the lift coefficient $c_{\mathrm{l}}(t)$ and the difference of the pressure between the front and the back of the cylinder

$$\Delta p(t) = p(t;0.15,0.2) - p(t;0.25,0.2)$$

The definition of $c_{\mathrm{d}}(t)$ and $c_{\mathrm{l}}(t)$ in Reference [6] is as follows:

$$c_{\mathrm{d}}(t) = \frac{2}{\rho L U_{\max}^2} \int_S \left(\rho \nu \frac{\partial \mathbf{u}_{t_S}(t)}{\partial n} n_y - p(t) n_x \right) \mathrm{d}S \tag{2}$$

$$c_{\mathrm{l}}(t) = -\frac{2}{\rho L U_{\max}^2} \int_S \left(\rho \nu \frac{\partial \mathbf{u}_{t_S}(t)}{\partial n} n_x + p(t) n_y \right) \mathrm{d}S \tag{3}$$

‡These pictures have been plotted with the software package GRAPE.

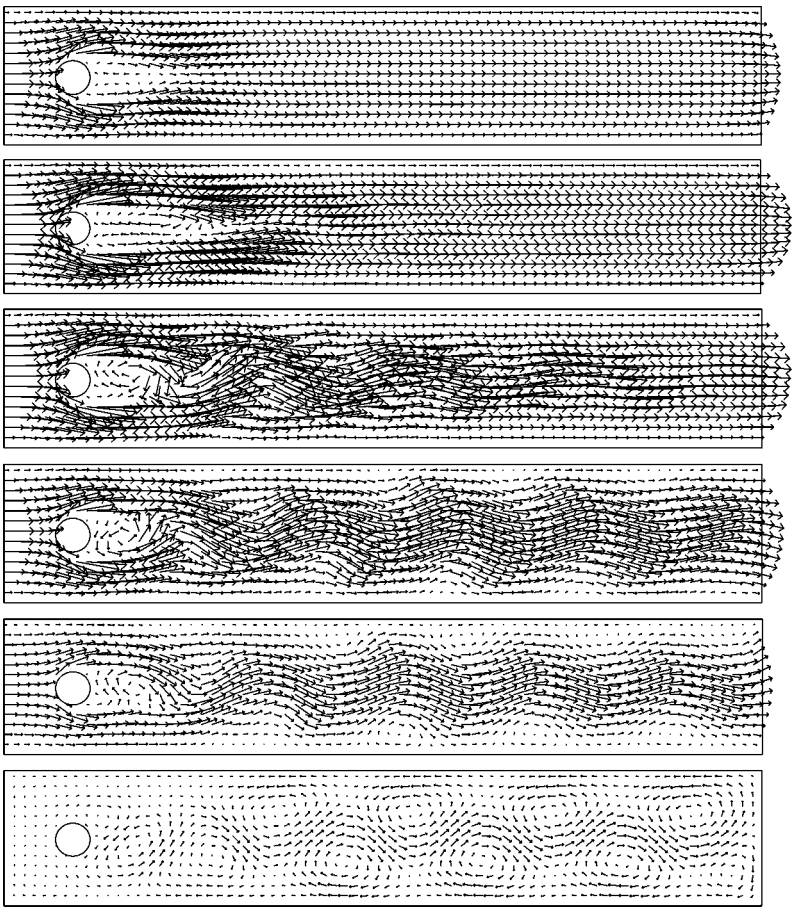

Figure 2. The velocity at times 2, 4, 5, 6, 7 and 8 s.

Here, $n=(n_x,n_y)^{\mathrm{T}}$ is the normal vector on S directing into Ω, $t_S=(n_y,-n_x)^{\mathrm{T}}$ the tangential vector and $\mathbf{u}_{t_S}$ the tangential velocity. A straightforward calculation gives

$$c_{\mathrm{d}}(t)=-20\int_{\Omega}[\nu\nabla\mathbf{u}(t):\nabla\mathbf{v}_{\mathrm{d}}+(\mathbf{u}(t)\cdot\nabla)\mathbf{u}(t)\cdot\mathbf{v}_{\mathrm{d}}-p(t)(\nabla\cdot\mathbf{v}_{\mathrm{d}})]\,\mathrm{d}x\,\mathrm{d}y \tag{4}$$

for all functions $\mathbf{v}_{\mathrm{d}}\in(H^1(\Omega))^2$ with $(\mathbf{v}_{\mathrm{d}})|_S=(1,0)^{\mathrm{T}}$ and $\mathbf{v}_{\mathrm{d}}$ vanishes on all other boundaries. Similarly, one obtains

$$c_{\mathrm{l}}(t)=-20\int_{\Omega}[\nu\nabla\mathbf{u}(t):\nabla\mathbf{v}_{\mathrm{l}}+(\mathbf{u}(t)\cdot\nabla)\mathbf{u}(t)\cdot\mathbf{v}_{\mathrm{l}}-p(t)(\nabla\cdot\mathbf{v}_{\mathrm{l}})]\,\mathrm{d}x\,\mathrm{d}y \tag{5}$$

for all test functions $\mathbf{v}_{\mathrm{l}}\in(H^1(\Omega))^2$ with $(\mathbf{v}_{\mathrm{l}})|_S=(0,1)^{\mathrm{T}}$ and $\mathbf{v}_{\mathrm{l}}$ vanishes on all other boundaries. We have the experience that the volume integral formulations (4), (5) are more accurate and less sensitive to the approximation of the circular boundary S than the line integral

formulations (2), (3), see Reference [9]. The actual choice of $\mathbf{v}_d$ and $\mathbf{v}_l$ in our computations is the same as in the steady-state problem investigated in Reference [4].

The evolutions of $c_d(t)$, $c_l(t)$ and $\Delta p(t)$ which were computed with very fine discretizations in time and space will be presented in Section 4. Since it is not possible to give the complete data of these curves as reference values, we will concentrate on one specific value for each parameter. As proposed in Reference [6], we take the maximal drag and lift coefficients together with the corresponding times and the final pressure difference $\Delta p(8\,\mathrm{s})$.

3. THE DISCRETIZATIONS

For discretizing system (1), we apply the following strategy:

1. *Discretization of* (1) *in time*: We will use a second-order implicit time stepping scheme. The time discretization leads in each discrete time step to a non-linear system of equations.
2. *Variational formulation and linearization*: The non-linear system of equations is reformulated as variational problem and the non-linear variational problem is linearized by a fixed point iteration.
3. *Discretization of the linear systems in space*: The linear system of equations arising in each step of the fixed point iteration is discretized by a second-order finite element discretization using an inf–sup stable pair of finite element spaces.

The temporal discretization which were applied in the computations are the Crank–Nicolson scheme and the fractional-step θ-scheme. These are popular time stepping schemes in CFD, e.g. see Reference [10]. The optimal order convergence of these schemes applied in the solution of the Navier–Stokes equations, also in connection with finite element discretizations in space, is proven, e.g. in References [11, 12].

Let Δt_n be the current time step from t_{n-1} to t_n, i.e. $\Delta t_n = t_n - t_{n-1}$. We denote quantities at time level t_k by a subscript k. The time step in both time stepping schemes has the form

$$\begin{aligned} &\mathbf{u}_k + \theta_1 \Delta t_n[-\nu\Delta\mathbf{u}_k + (\mathbf{u}_k \cdot \nabla)\mathbf{u}_k] + \Delta t_k \nabla p_k \\ &\quad = \mathbf{u}_{k-1} - \theta_2 \Delta t_n[-\nu\Delta\mathbf{u}_{k-1} + (\mathbf{u}_{k-1} \cdot \nabla)\mathbf{u}_{k-1}] + \theta_3 \Delta t_n \mathbf{f}_{k-1} + \theta_4 \Delta t_n \mathbf{f}_k \\ &\nabla \cdot \mathbf{u}_k = 0 \end{aligned} \tag{6}$$

with the parameters $\theta_1, \ldots, \theta_4$. The Crank–Nicolson scheme is given by $\theta_1 = \theta_2 = \theta_3 = \theta_4 = 0.5$, $t_{k-1} = t_{n-1}$, $\Delta t_k = \Delta t_n$ and $t_k = t_n$. The fractional-step θ-scheme is obtained by three steps of form (6). The parameters for these steps are given in Table I, where

$$\theta = 1 - \frac{\sqrt{2}}{2}, \quad \tilde{\theta} = 1 - 2\theta, \quad \tau = \frac{\tilde{\theta}}{1-\theta}, \quad \eta = 1 - \tau$$

System (6) is reformulated as a non-linear variational problem in time step t_k. This problem is solved iteratively by a fixed point iteration. Let $(\mathbf{u}_k^0, p_k^0)$ be an initial guess. Given $(\mathbf{u}_k^m, p_k^m)$,

Table I. Parameters for the fractional-step θ-scheme.

	θ_1	θ_2	θ_3	θ_4	t_{k-1}	t_k	Δt_k
First substep	$\tau\theta$	$\eta\theta$	$\eta\theta$	$\tau\theta$	t_{n-1}	$t_{n-1}+\theta\,\Delta t_n$	$\theta\,\Delta t_n$
Second substep	$\eta\tilde{\theta}$	$\tau\tilde{\theta}$	$\tau\tilde{\theta}$	$\eta\tilde{\theta}$	$t_{n-1}+\theta\,\Delta t_n$	$t_n-\theta\,\Delta t_n$	$\tilde{\theta}\,\Delta t_n$
Third substep	$\tau\theta$	$\eta\theta$	$\eta\theta$	$\tau\theta$	$t_n-\theta\,\Delta t_n$	t_n	$\theta\,\Delta t_n$

the iterate $(\mathbf{u}_k^{m+1}, p_k^{m+1})$ is computed by solving

$$\begin{aligned}
&(\mathbf{u}_k^{m+1},\mathbf{v})+\theta_1\,\Delta t_n[\nu(\nabla\mathbf{u}_k^{m+1},\nabla\mathbf{v})+((\mathbf{u}_k^{m}\cdot\nabla)\mathbf{u}_k^{m+1},\mathbf{v})]-\Delta t_k(p_k^{m+1},\nabla\cdot\mathbf{v})\\
&\quad=(\mathbf{u}_{k-1},\mathbf{v})-\theta_2\Delta t_n[(\nu\nabla\mathbf{u}_{k-1},\nabla\mathbf{v})+((\mathbf{u}_{k-1}\cdot\nabla)\mathbf{u}_{k-1},\mathbf{v})]\\
&\qquad+\theta_3\Delta t_n(\mathbf{f}_{k-1},\mathbf{v})+\theta_4\Delta t_n(\mathbf{f}_k,\mathbf{v}),\quad \forall\mathbf{v}\in(H_0^1(\Omega))^2\\
&0=(\nabla\cdot\mathbf{u}_k^{m+1},q)\quad \forall q\in L_0^2(\Omega)
\end{aligned}\tag{7}$$

$m=0,1,2,\ldots$. Here, $L_0^2(\Omega)$ is the space of all functions in $L^2(\Omega)$ with $\int_\Omega q\,\mathrm{d}x\,\mathrm{d}y=0$.

The linear system (7) is discretized by a second order, isoparametric and inf–sup stable pair of finite elements. On a quadrilateral grid, we use the mapped Q_2/P_1^{disc} finite element, i.e. the velocity is approximated by continuous piecewise biquadratics and the pressure by discontinuous piecewise linears on a reference mesh cell. The finite element on a mesh cell in Ω is given by the reference map from the reference mesh cell. The inf–sup stability for the mapped version of this pair of finite elements has been proven recently in Reference [13]. On a triangular grid, we use the P_2/P_1 finite element (Taylor–Hood element). The use of isoparametric finite elements, which provide a better approximation of the curved boundary S than standard finite elements, has been proven essential to compute accurate drag and lift coefficients in steady state flows around a cylinder, see References [4, 5].

4. EVALUATION OF THE COMPUTATIONAL RESULTS

Computations were carried out on different refinement levels of the spatial grid and with different lengths of the equidistant time step. The complete results are given in Tables III–VI.

The initial spatial quadrilateral and triangular grid (level 0) are presented in Figure 3 and the corresponding numbers of degrees of freedom on different refinement levels in Table II.

The fixed point iteration (7) for solving the non-linear system in each time step was stopped if the Euclidean norm of the residual vector was less than $1e-10$. With this very accurate solution of the non-linear problems, we tried to minimize the influence of the error committed by stopping the fixed point iteration on the computed parameters. For the combination of the Crank–Nicolson scheme with $\Delta t_n=0.04$ and the P_2/P_1 finite element discretization, it was not possible to fulfil this stopping criterion for every discrete time. That is why, no results are reported for these computations in Table VI. For solving the linear systems, we used a flexible GMRES method with a multiple discretization multilevel method as preconditioner, see Reference [5] for details.

The evolution of $c_{\mathrm{d}}(t)$, $c_{\mathrm{l}}(t)$ and $\Delta p(t)$ is presented in Figure 4. For defining reference values for the maximal drag $c_{\mathrm{d,max}}$, the maximal lift $c_{\mathrm{l,max}}$ and $\Delta p(8\,\mathrm{s})$, we consider only the

Table II. Number of degrees of freedom on different refinement levels.

	Q_2/P_1^{disc}			P_2/P_1		
Level	Velocity	Pressure	Total	Velocity	Pressure	Total
1	6960	2496	9456	6496	848	7344
2	27 232	9984	37 216	25 408	3248	28 656
3	107 712	39 936	147 648	100 480	12 704	113 184
4	428 416	159 744	588 160	399 616	50 240	449 856

Table III. Fractional-step θ-scheme and Q_2/P_1^{disc} finite element discretization.

Level	Δt_k	$t(c_{\text{d,max}})$	$c_{\text{d,max}}$	$t(c_{\text{l,max}})$	$c_{\text{l,max}}$	$\Delta p(8\text{ s})$
1	0.04	3.92	*2.9506391*	5.92	0.40715733	−0.11033257
1	0.02	3.94	*2.9507340*	5.9	0.41665841	−0.10949532
1	0.01	3.93	*2.9507247*	5.89	0.41920611	−0.10915065
1	0.005	3.935	*2.9507228*	5.89	0.41963964	−0.10907600
1	0.00025	3.935	*2.9507167*	5.8875	0.41969340	−0.10910838
1	0.000125	3.93375	*2.9507161*	5.88875	0.41970676	−0.10914699
2	0.04	3.92	*2.9508005*	5.72	0.46735721	−0.10933540
2	0.02	3.94	*2.9509575*	5.72	*0.48088381*	*−0.11135376*
2	0.01	3.94	*2.9509598*	5.71	0.48567099	*−0.11168681*
2	0.005	3.935	*2.9509514*	5.705	0.48674228	*−0.11180484*
2	0.0025	3.9375	*2.9509474*	5.705	0.48677266	*−0.11186812*
2	0.00125	3.93625	*2.9509476*	5.70375	0.48679031	*−0.11191150*
3	0.04	3.92	*2.9507807*	5.72	0.46668809	*−0.11051418*
3	0.02	3.94	*2.9509409*	5.7	*0.47595858*	*−0.11141326*
3	0.01	3.94	*2.9509414*	5.7	*0.47696648*	*−0.11145178*
3	0.005	3.935	*2.9509362*	5.695	*0.47833933*	*−0.11152352*
3	0.0025	3.9375	*2.9509283*	5.6925	*0.47841502*	*−0.11158920*
3	0.00125	3.93625	*2.9509232*	5.69375	*0.47838978*	*−0.11161155*
4	0.04	3.92	*2.9507765*	5.72	0.46624734	*−0.11053528*
4	0.02	3.94	*2.9509386*	5.7	*0.47551966*	*−0.11141362*
4	0.01	3.94	*2.9509292*	5.7	*0.47641039*	*−0.11150460*
4	0.005	3.935	*2.9509241*	5.695	*0.47785984*	*−0.11149907*
4	0.0025	3.9375	*2.9509219*	5.6925	*0.47797551*	*−0.11160224*
*4	0.00125	3.93625	*2.9509220*	5.6925	*0.47797321*	*−0.11163948*

computations with the finest discretizations in Tables III–VI (marked with an asterisk). The following reference intervals are given in Reference [6]:

$$c_{\text{d,max}}^{\text{ref}} \in [2.93, 2.97], \quad c_{\text{l,max}}^{\text{ref}} \in [0.47, 0.49], \quad \Delta p^{\text{ref}}(8\text{ s}) \in [-0.115, -0.105]$$

The maximal drag coefficient is the least sensitive of the parameters of interest. It is computed with both time stepping schemes and with both spatial discretizations at the same discrete time and the six leading digits are in all four cases the same. We propose to take

Table IV. Fractional-step θ-scheme and P_2/P_1 finite element discretization.

Level	Δt_k	$t(c_{\mathrm{d,max}})$	$c_{\mathrm{d,max}}$	$t(c_{\mathrm{l,max}})$	$c_{\mathrm{l,max}}$	$\Delta p(8\,\mathrm{s})$
1	0.04	3.92	*2.9528222*	6.12	0.28268683	−0.11021790
1	0.02	3.94	*2.9528819*	6.08	0.29192437	−0.10863794
1	0.01	3.93	*2.9528799*	6.08	0.29548536	−0.10822905
1	0.005	3.935	*2.9528380*	6.08	0.29607335	−0.10817002
1	0.0025	3.935	*2.9528602*	6.08	0.29615308	−0.10820374
1	0.00125	3.93375	*2.9528498*	6.08	0.29633652	−0.10823178
2	0.04	3.92	*2.9507820*	5.76	0.46134147	−0.10668118
2	0.02	3.94	*2.9509452*	5.72	*0.47597790*	−0.10998301
2	0.01	3.93	*2.9509371*	5.72	*0.48048129*	*−0.11075046*
2	0.005	3.935	*2.9509319*	5.72	*0.48103846*	*−0.11104868*
2	0.0025	3.9375	*2.9509593*	5.72	*0.48116515*	*−0.11090129*
2	0.00125	3.9	2.9541462	5.71875	*0.48108260*	*−0.11110045*
3	0.04	3.92	*2.9508632*	5.72	0.46673290	−0.11043995
3	0.02	3.94	*2.9509351*	5.7	*0.47600081*	*−0.11143063*
3	0.01	3.94	*2.9509555*	5.7	*0.47755069*	*−0.11151841*
3	0.005	3.935	*2.9509291*	5.695	*0.47870779*	*−0.11157032*
3	0.0025	3.9375	*2.9509245*	5.695	*0.47877711*	*−0.11153602*
3	0.00125	3.93625	*2.9509240*	5.69375	*0.47873533*	*−0.11164246*
4	0.04	3.92	*2.9507778*	5.72	0.46626260	*−0.11053065*
4	0.02	3.94	*2.9509481*	5.7	*0.47548079*	*−0.11138078*
4	0.01	3.94	*2.9509307*	5.7	*0.47642030*	*−0.11146902*
4	0.005	3.935	*2.9509209*	5.695	*0.47799101*	*−0.11151052*
4	0.0025	3.9375	*2.9509231*	5.6925	*0.47814399*	*−0.11146390*
*4	0.00125	3.93625	*2.9509216*	5.6925	*0.47811979*	*−0.11158097*

the average of the four values as reference value. This gives

$$t(c_{\mathrm{d,max}}^{\mathrm{ref}}) = 3.93625, \quad c_{\mathrm{d,max}}^{\mathrm{ref}} = 2.950921575 \tag{8}$$

From the computational results can be deduced that the error of $c_{\mathrm{d,max}}^{\mathrm{ref}}$ to the true value is less than $5e-7$.

The results for the maximal lift coefficient among the four computations with the finest discretizations are not as equal as for the drag coefficient. In the computations with the fractional-step θ-scheme, $c_{\mathrm{l,max}}$ is obtained at 5.6925 s whereas using the Crank–Nicolson scheme, it is obtained one time step later. The difference between the smallest and the largest value for $c_{\mathrm{l,max}}$ is about $2e-4$. The values obtained on the triangular grid are larger than the values obtained on the quadrilateral grid. The fineness of the spatial grid has more influence on $c_{\mathrm{l,max}}$ than the fineness of the time step. Considering $\Delta t_n = 0.00125$, the numerical order of convergence for $c_{\mathrm{l,max}}$ computed with the values on levels 2–4 is approximately 4 on the quadrilateral grid and approximately 2 on the triangular grid. Extrapolations of the values on level 4 with these orders yield $c_{\mathrm{l,max}} \in [0.4779, 0.4780]$. We take the centre of this interval as reference value

$$t(c_{\mathrm{l,max}}^{\mathrm{ref}}) = 5.693125, \quad c_{\mathrm{l,max}}^{\mathrm{ref}} = 0.47795 \tag{9}$$

Table V. Crank–Nicolson scheme and Q_2/P_1^{disc} finite element discretization.

Level	Δt_k	$t(c_{\text{d,max}})$	$c_{\text{d,max}}$	$t(c_{\text{l,max}})$	$c_{\text{l,max}}$	$\Delta p(8\text{ s})$
1	0.04	3.96	*2.9505083*	6.08	0.32464525	−0.10018096
1	0.02	3.94	*2.9506817*	5.94	0.39561339	−0.10857361
1	0.01	3.94	*2.9507128*	5.9	0.41374429	−0.10955200
1	0.005	3.935	*2.9507191*	5.895	0.41871121	−0.10908404
1	0.0025	3.935	*2.9507186*	5.89	0.41966279	−0.10903674
1	0.00125	3.93375	*2.9507178*	5.88875	0.41977686	−0.10909697
2	0.04	3.96	*2.9505154*	5.92	0.38267229	−0.10408771
2	0.02	3.94	*2.9508259*	5.76	0.46347330	−0.10483694
2	0.01	3.94	*2.9509214*	5.72	*0.48183570*	*−0.11055802*
2	0.005	3.935	*2.9509429*	5.71	0.48592837	*−0.11142277*
2	0.0025	3.94	*2.9509537*	5.705	0.48675826	*−0.11167859*
2	0.00125	3.93625	*2.9509487*	5.705	0.48684486	*−0.11182187*
3	0.04	3.96	*2.9505770*	5.88	0.38547587	−0.10218613
3	0.02	3.94	*2.9508121*	5.74	0.45313392	−0.10682960
3	0.01	3.94	*2.9508996*	5.71	*0.47341914*	*−0.11096780*
3	0.005	3.94	*2.9509211*	5.7	*0.47744148*	*−0.11127794*
3	0.0025	3.9375	*2.9509263*	5.695	*0.47843334*	*−0.11139759*
3	0.00125	3.93625	*2.9509266*	5.69375	*0.47851502*	*−0.11150848*
4	0.04	3.96	*2.9507127*	5.88	0.38520920	−0.10215215
4	0.02	3.94	*2.9508480*	5.74	0.45281094	−0.10686868
4	0.01	3.94	*2.9508913*	5.71	0.47292459	*−0.11097007*
4	0.005	3.94	*2.9509159*	5.7	*0.47693587*	*−0.11126441*
4	0.0025	3.9375	*2.9509213*	5.695	*0.47797207*	*−0.11136252*
*4	0.00125	3.93625	*2.9509212*	5.69375	*0.47805421*	*−0.11150005*

The computational results suggest that the difference of $c_{\text{l,max}}^{\text{ref}}$ to the true value is not larger than $1e-4$.

For $\Delta p(8\text{ s})$, the leading three digits are the same in all four computations. The values obtained with the fractional-step θ-scheme are a little bit less than the values obtained with the Crank–Nicolson scheme. The fineness of the time step seems to influence $\Delta p(8\text{ s})$ more than the fineness of the spatial level. On level 4, there is the tendency that $\Delta p(8\text{ s})$ decreases the finer the time step becomes. Defining the reference value by

$$\Delta p^{\text{ref}}(8s) = -0.1116 \tag{10}$$

the computed values lead to the conjecture that the deviation from the real value is less than $1e-4$.

The four computations which were used to determine the reference values give very similar results not only for these values but in the whole time interval. The maximal difference in $[0,8]$ of $c_{\text{d}}(t)$ between any of these computations is about $2.45e-3$, of $c_{\text{l}}(t)$ is $4.38e-3$ and of $\Delta p(t)$ is $1.89e-3$.

In Tables III–VI, all coefficients are emphasized whose relative error is less than 0.1% for the drag coefficient and less than 1% for the lift coefficient and the pressure difference. It can be seen that there are only minor differences between the results obtained with both time stepping schemes. Only for large time steps, the fractional-step θ-scheme gives more accurate

Table VI. Crank–Nicolson scheme and P_2/P_1 finite element discretization.

Level	Δt_k	$t(c_{\mathrm{d,max}})$	$c_{\mathrm{d,max}}$	$t(c_{\mathrm{l,max}})$	$c_{\mathrm{l,max}}$	$\Delta p(8\,\mathrm{s})$
1	0.02	3.94	*2.9528629*	6.14	0.27500061	−0.10997106
1	0.01	3.94	*2.9528743*	6.1	0.29101136	−0.10882587
1	0.005	3.935	*2.9528769*	6.085	0.29516392	−0.10817065
1	0.0025	3.935	*2.9528739*	6.0825	0.29604608	−0.10810506
1	0.00125	3.93375	*2.9528735*	6.08	0.29622602	−0.10821017
2	0.02	3.94	*2.9508028*	5.78	0.45611390	−0.10178337
2	0.01	3.94	*2.9508900*	5.73	*0.47502698*	−0.10873577
2	0.005	3.935	*2.9509017*	5.725	*0.48020958*	−0.11034456
2	0.0025	3.9375	*2.9509065*	5.72	*0.48096861*	*−0.11082242*
2	0.00125	3.93625	*2.9509085*	5.72	*0.48117740*	*−0.11100239*
3	0.02	3.98	*2.9516650*	5.74	0.45192747	−0.10667705
3	0.01	3.94	*2.9508963*	5.71	*0.47369666*	*−0.11096193*
3	0.005	3.935	*2.9509249*	5.7	*0.47777323*	*−0.11132001*
3	0.0025	3.9375	*2.9509237*	5.695	*0.47856834*	*−0.11146826*
3	0.00125	3.93625	*2.9509252*	5.695	*0.47882390*	*−0.11156480*
4	0.02	3.94	*2.9508519*	5.74	0.45281283	−0.10686458
4	0.01	3.94	*2.9508915*	5.71	*0.47293898*	*−0.11097224*
4	0.005	3.935	*2.9509534*	5.7	*0.47694264*	*−0.11125744*
4	0.0025	3.9375	*2.9509225*	5.695	*0.47804047*	*−0.11141205*
*4	0.00125	3.93625	*2.9509215*	5.69375	*0.47814971*	*−0.11150381*

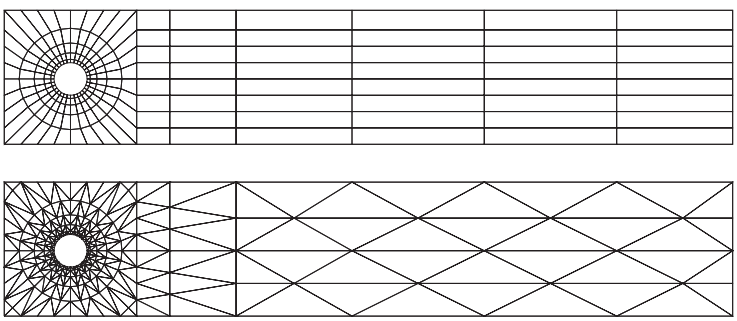

Figure 3. Coarsest grids for the computations (level 0).

results. This observation corresponds with the statements in Reference [10, Section 3.2.2]. Also the quality of the results on the quadrilateral and the triangular grid is very similar.

We like to note that using a first-order discretization in space or in time yields much more inaccurate results. A study with the first-order non-conforming Crouzeix–Raviart finite element discretization and the Crank–Nicolson scheme as time stepping method in Reference [9] gave as best results

$$c_{\mathrm{d,max}} = 2.9749, \quad c_{\mathrm{l,max}} = 0.4808, \quad \Delta p(8\,\mathrm{s}) = -0.1011$$

These results were obtained with about 785 000 degrees of freedom in space and with $\Delta t_n = 0.0025$. Using the first-order backward Euler scheme as time discretization ($\theta_1 = \theta_4 = 1$,

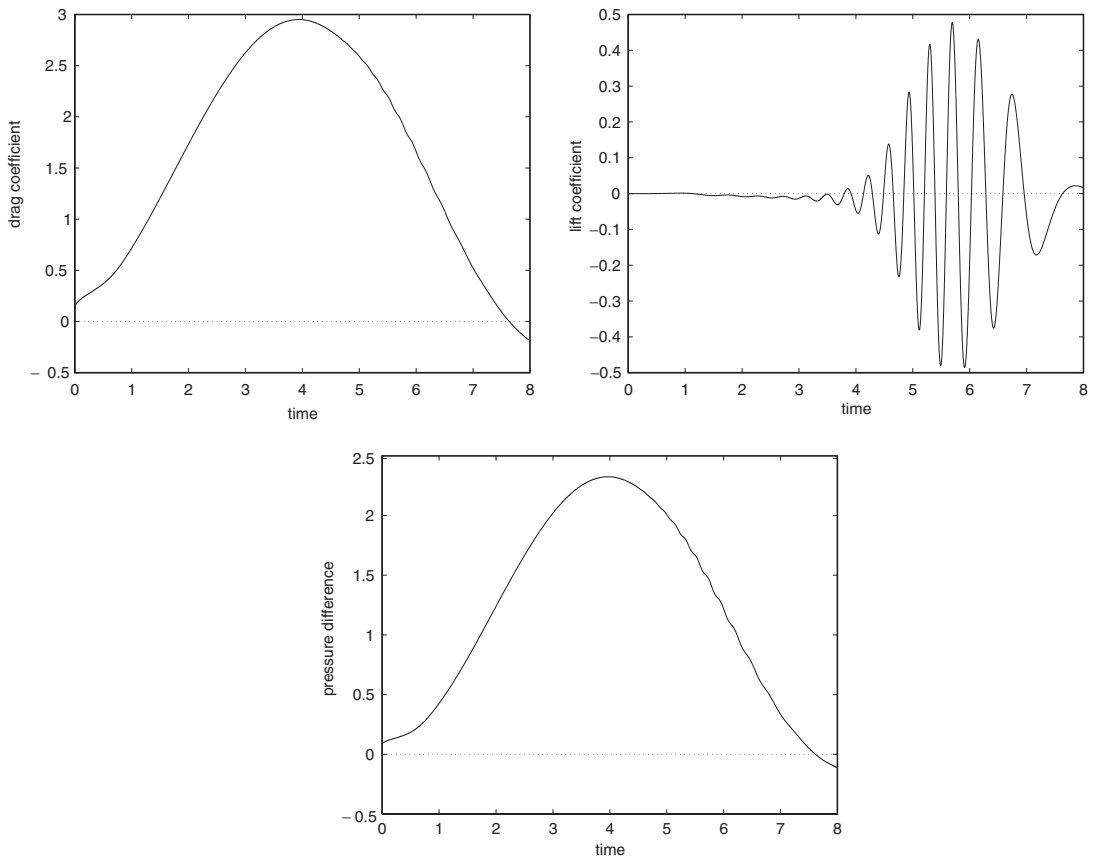

Figure 4. Evolution of $c_{\mathrm{d}}(t)$, $c_{\mathrm{l}}(t)$ and $\Delta p(t)$.

$\theta_2 = \theta_3 = 0, \Delta t_k = \Delta t_n$ in (6)) with $\Delta t_n = 0.00125$ and the Q_2/P_1^{disc} finite element discretization on level 4 gives

$$t(c_{\mathrm{d,max}}) = 3.93375, \quad c_{\mathrm{d,max}} = 2.9505567$$

$$t(c_{\mathrm{l,max}}) = 5.7175, \quad c_{\mathrm{l,max}} = 0.38212635$$

$$\Delta p(8\ \mathrm{s}) = -0.11134512$$

Whereas the results for $c_{\mathrm{d,max}}$ and $\Delta p(8\mathrm{s})$ are rather close to the reference values, the maximal lift coefficient is computed very inaccurately.

5. SUMMARY

A two-dimensional flow through a channel around a cylinder with a time-dependent inflow was computed with two different second-order implicit time stepping schemes and two different

second-order finite element discretizations. The evolutions of the drag and the lift coefficient at the cylinder and the pressure difference between the front and the back of the cylinder have been studied. Using about 500 000 degrees of freedom in space and an equidistant time step of $\Delta t_n = 0.00125$, the results with the four combinations of these schemes show very similar results. New reference values for the maximal drag coefficient, (8), the maximal lift coefficient, (9), and the pressure difference at the final time, (10), have been derived from the computational results.

REFERENCES

1. Ghia U, Ghia KN, Shin CT. High-*Re* solutions for incompressible flows using the Navier–Stokes equations and a multigrid method. *Journal of Computational Physics* 1982; **48**:387–411.
2. Gartling DK. A test problem for outflow boundary conditions—flow over a backward-facing step. *International Journal for Numerical Methods in Fluids* 1990; **11**:953–967.
3. Nabh G. On higher order methods for the stationary incompressible Navier–Stokes equations. *Ph.D. Thesis*, Universität Heidelberg, 1998, Preprint 42/98.
4. John V, Matthies G. Higher order finite element discretizations in a benchmark problem for incompressible flows. *International Journal for Numerical Methods in Fluids* 2001; **37**:885–903.
5. John V. Higher order finite element methods and multigrid solvers in a benchmark problem for the 3D Navier–Stokes equations. *International Journal for Numerical Methods in Fluids* 2002; **40**:775–798.
6. Schäfer M, Turek S. The benchmark problem 'flow around a cylinder'. In *Flow Simulation with High-Performance Computers II*, Hirschel EH (ed.). Notes on Numerical Fluid Mechanics, vol. 52. Vieweg: Braunschweig, 1996; 547–566.
7. Galdi GP. An introduction to the Navier–Stokes initial-boundary value problem. In *Fundamental Directions in Mathematical Fluid Dynamics*, Galdi GP, Heywood JG, Rannacher R (eds). Basel: Birkhäuser; 2000; 1–70.
8. Sohr H. *The Navier–Stokes Equations, An Elementary Functional Analytic Approach*. Birhäuser Advanced Texts. Birkhäuser Verlag: Basel, Boston, Berlin, 2001.
9. John V. Parallele Lösung der inkompressiblen Navier–Stokes Gleichungen auf adaptiv verfeinerten Gittern. *Ph.D. Thesis*, Otto-von-Guericke-Universität Magdeburg, Fakultät für Mathematik, 1997.
10. Turek S. *Efficient Solvers for Incompressible Flow Problems: An Algorithmic and Computational Approach*. Lecture Notes in Computational Science and Engineering, vol. 6. Springer: Berlin, 1999.
11. Heywood JG, Rannacher R. Finite element approximation of the nonstationary Navier–Stokes problem IV: Error analysis for second order time discretizations. *SIAM Journal on Numerical Analysis* 1990; **27**:353–384.
12. Müller-Urbaniak S. *Eine Analyse des Zwischenschritt-θ-Verfahrens zur Lösung der instationären Navier–Stokes-Gleichungen*. Preprint 94-01, Universität Heidelberg, Interdisziplinäres Zentrum für wissenschaftliches Rechnen, 1994.
13. Matthies G, Tobiska L. The inf–sup condition for the mapped $Q_k/P_{k-1}^{\mathrm{disc}}$ element in arbitrary space dimensions. *Computing* 2002; **69**:119–139.

